IEEE *Access*
Multidisciplinary : Rapid Review : Open Access Journal

Potential Applicability of SMAP in ECV Soil Moisture Gap-filling: A Case Study in Europe (May 2020)

Yangxiaoyue Liu [1, 2], Yaping Yang [3, 4] and Wenlong Jing [1, 2]

[1]Guangdong Open Laboratory of Geospatial Information Technology and Application, Key Laboratory of Guangdong for Utilization of Remote Sensing and Geographical Information System, Engineering Technology Center of Remote Sensing Big Data Application of Guangdong Province, Guangzhou Institute of Geography, Guangzhou 510070, China

[2] Southern Marine Science and Engineering Guangdong Laboratory, Guangzhou 511458, China

[3] State Key Laboratory of Resources and Environmental Information System, Institute of Geographic Sciences and Natural Resources Research, Chinese Academy of Sciences, Beijing 100101, China

[4] Jiangsu Center for Collaborative Innovation in Geographical Information Resource Development and Application, Nanjing Normal University, Nanjing 210023, China

Corresponding author: Yaping Yang (yangyp@igsnrr.ac.cn).

ABSTRACT The Essential Climate Variable (ECV) soil moisture (SM) datasets, originated from the European Space Agency, have revealed great potential for application in hydrology and agriculture. Hence, it is essential to continuously enhance the data quality and spatial completeness to satisfy the increasing scientific research requirements. In this study, we explore the potential possibility of Soil Moisture Active Passive (SMAP) datasets in filling the gaps of ECV SM. The comprehensive assessment results show that: (1) The data missing percent of gap-filled ECV decreases 20% on average, which can be one step closer to generate a seamlessly covered global land surface SM product with favorable quality. (2) Compared to the original ECV, the gap-filled ECV products express similar good response to the in-situ measurements, suggesting that the SMAP SM products could be taken to efficiently fill the gaps and consistently maintain favorable accuracy at the same time. (3) Compared to the in-situ measurements, the original ECV SM products demonstrate extremely high probability density peak percentages. Fortunately, this eminent high value could be effectively rectified through gap-filling progress using SMAP. Overall, this study conducts objective and detailed evaluation on the performance of applying SMAP to fill the gaps of ECV, and is expected to act as a valuable reference in ECV SM gap-filling method.

INDEX TERMS gap-filling, satellite retrieved soil moisture, the Essential Climate Variable soil moisture, the Soil Moisture Active Passive soil moisture

I. INTRODUCTION

Land surface soil moisture (SM), acting as an important vector in underlying surface hydrothermal exchange, is a key element in reflecting root-zone SM conditions and feeding the growth of herbaceous plants [1-3]. Moreover, spatio-temporal SM data is considered as critical references in land-atmosphere interactions, vapor circulation, crop growth monitoring, and watershed hydrological process across the globe [4, 5]. Consequently, it is increasingly vital to acquire

high-accuracy SM products with continuous land surface coverage to promote public awareness about the near surface topsoil hydrological situation [6, 7].

Meanwhile, satellite-based remote sensing technology is advancing rapidly and becoming an efficient way to acquire large scale spectral information [8-13]. With various microwave sensors on-board Earth observation satellites, daily SM can be derived by radiation transfer equations and

backscattering models via signals received by satellite [14]. According to different working modes, satellite-based sensors are mainly divided into active instruments (laser radar, doppler radar, synthetic aperture radar) and passive instruments (microwave radiometer, multi-spectral imager, imaging spectrometer) [15, 16].

Substantial efforts have been made to obtain SM by active instruments [17-19]. The Japan Aerospace Exploration Agency launched the Advanced Land Observation Satellite-Phased Array type L-band Synthetic Aperture Radar (ALOS-PALSAR), which is an L-band synthetic aperture radar (SAR) product, to perform all-weather SM monitoring under three working modes, called the fine, scanning SAR, and polarimetric modes [17]. The European Space Agency (ESA) designed and developed the European Remote Sensing (ERS-1/2) satellites in the 1990s to measure daily SM [18]. Moreover, the ESA also initiated the Sentinel-1 satellite system with C-band SAR onboard to collect continuous active microwave data to derive SM [19].

Similarly, passive sensors are universally used for obtaining SM signals [20-22]. The solar synchronous satellite EOS-Aqua, launched by the National Space Development Agency of Japan (NASDA), is equipped with the advanced microwave scanning radiometer Earth observing system (AMSR-E) [20]. Composed of six bands from 6.9-89 GHz, SM was inversed through a 10.7 GHz band signal. Then, AMSR2 continues collecting brightness temperature after AMSR-E completes its service in 2012 [21]. The ESA initiates the Soil Moisture and Ocean Salinity (SMOS) plan, aiming to observe SM and ocean salinity simultaneously. The 1.4 GHz signals received by synthetic aperture radiometer on the SMOS satellite can penetrate 5 cm deep into soil and no more than 5 kg/m^2 water content of vegetation cover [22].

In general, both active and passive sensors are verified to have promising potential for SM retrieval. Additionally, each working mode sensor has its own characteristics. Active microwave sensors usually acquire data with high spatial resolution (tens of meters) but long revisit period (16-25 days). Passive microwave sensors can obtain daily global signals, but have coarse spatial resolution. Additionally, as SAR has high backscattering frequency, the accuracy of SAR-derived SM in vegetation-covered areas and crop fields is remarkably lower than that in bare areas. Therefore, passive SM is more frequently utilized in SM analysis in mixed land cover and large-scale regions.

To take advantage of both active and passive SM products, research institutions tries to develop multi-sensor combined SM by fusing active and passive sensor-derived SM dataset. Since 2010, the ESA, after launching the Climate Change Initiative project, is devoted to developing high-precision SM products called the Essential Climate Variable (ECV) SM [23, 24]. This program merges currently available SM products and obtained a 0.25° resolution, daily SM product from 1st November 1978 to now. The ECV SM contains three datasets: (1) Active ECV SM (ECV_A), through merging ERS-1/2 [25] and METeorological OPerational satellite (MetOp-A/B) [26] scatterometer derived SM; (2) Passive ECV SM (ECV_P),

through merging Scanning Multichannel Microwave Radiometer (SMMR) [27], Special Sensor Microwave/Imager (SSM/I) [28], Tropical Rainfall Mission Microwave Image (TMI) [29], AMSR-E/2 [1, 6, 30], Windsat [31], and SMOS [32] radiometer-based SM; and (3) Active and passive combined ECV SM (ECV_C), through merging ECV_A and ECV_P.

Many studies have made extraordinary contributions to assess the quality of the ECV SM [4, 23, 33-37]. Most of their results suggested that the ECV SM, especially ECV_C SM, outperformed numerous of traditional single-sensor retrieved SM products in both value accuracy and correlation coefficient. Further, to some extent, these findings approved the superiority of multi-active and passive sensors integrated ECV SM. However, although ECV SM has gained superior quality over many single-sensor retrieved SM products, more development is needed; not only to further improve data accuracy in diverse land cover types, but also to fill the gap areas to formulate a global completely covered land surface SM in a true sense. Previous studies utilized various of algorithms to reproduce SM in the gap regions [38-41], however, the robustness and applicability of each algorithm still need further discussions. It is suggested that with more members contributing, the spatial coverage integrity and data accuracy of ECV may get a chance for steady improvement. In addition, combining SM signals derived from various satellite-based sensors may have the potential to offer improved estimations of surface SM at a global scale [42, 43]. Hence, there exists an urgent need to explore the potential applicability of other highly-qualified satellite-based SM in ECV SM gap-filling.

Currently, as the satellite on-board sensor technology is increasingly maturing, new microwave-derived SM products are emerging continuously [44, 45]. The National Aeronautics and Space Administration (NASA) initiated the Soil Moisture Active Passive (SMAP) mission in January 2015, aiming to acquire global SM with intermediate resolution [46, 47]. It used both L-band radar and radiometer for concurrent, coincident SM measurements. The effectiveness of SMAP SM has gone through all-around validations since its inception [15, 48-50]. On average, SMAP SM compares very well against in-situ observations over different landcover types, except for dense vegetation areas like forest.

In general, increasing satellite-based SM appeared with improved and advanced instruments, which provide a promising opportunity for formulating a spatial completely covered ECV SM. As a result, in this study, an attempt is made to examine the potential applicability of SMAP in ECV SM gap filling with a case study in Europe.

II. DATA RESOURCES AND GAP-FILLING METHOD

A. SATELLITE RETRIEVED SM PRODUCTS
1) ECV SM
The ECV SM has approximately 40 years of top layer soil humidity data with global coverage, which could be a meaningful dataset for land-air hydrothermal transfer analysis

[51, 52]. Additionally, its time series keep extending with version renewal. This daily, 0.25° pixel-size dataset has been proved effectively in depicting large-scale hydrological evolution trends and drought spatial distribution levels worldwide [23]. In terms of the unique features of sensor operation modes, the ECV SM products are divided into three types: active sensor integrated ECV_A, passive sensor formulated ECV_P, and active passive sensor combined ECV_C. To carry out comparisons and explorations under different sensor modes, both ECV_P and ECV_C SM products were acquired from the official website (https://esa-soilmoisture-cci.org) to carry out the experiments.

Additionally, the ECV SM retrieving algorithms merge pre-processed level 2 SM products originated from radiometrically calibrated backscatter or brightness temperature measurements. Then, all these datasets are scaled against the Global Land Data Assimilation System Noah land surface model to harmonize their climatology. And the vegetation optical depth pattern derived uncertainty estimations are carry out to construct error covariance matrices. The correlation significance levels are used to mask out unreliable input elements, and the elements with favorable quality are merged to generate ECV_C and ECV_P [23, 43, 53-55].

In comparison, the unit of SM in ECV_C and ECV_P is m^3/m^3, while in ECV_A is % [34]. There exists a conversion formula between soil volumetric moisture content (m^3/m^3) and relative soil humidity (%) [56], shown by Equation (1). Since the SMAP SM belongs to passive microwave derived products with the unit of volumetric moisture content, we select the ECV_C and ECV_P to participate in the analysis in our research.

$$\theta_v = S_m \rho \theta_g \qquad (1)$$

where θ_v, S_m, ρ and θ_g stand for soil volumetric moisture content, relative soil humidity, soil bulk density and field moisture capacity, respectively.

2) SMAP SM

NASA launched the SMAP satellite successfully with an L-band radar and an L-band radiometer on-board on 31st January 2015 [57]. The SMAP program planned to measure daily SM by active and passive microwave sensors at 3 km and 36 km spatial resolutions, individually [48]. According to satellite orbit lifting and declining, the derived SMs are correspondingly named as ascending and descending products. However, the radar failed to deliver data since 7th July 2015. Therefore, the radiometer based 36 km SM and the enhanced radiometer 9 km SM are selected and evaluated in this study

to explore their potential applicability in filling the gaps of ECV SM. The SMAP SM dataset is released by the National Snow & Ice Data Center (NSIDC, https://nsidc.org/data/smap/smap-data.html).

The 36 km SMAP SM is retrieved from the detected brightness temperature signals from passive radiometer without further interpolation. Comparatively, the enhanced 9 km SMAP SM is derived from the SMAP Level 1B brightness temperature. The Backus Gilbert optimal interpolation algorithm is applied for comprehensive correction to form the enhanced bright temperature product. Then, the 9 km grid enhanced brightness temperature data is used as the main input data to retrieve the 9 km passive enhanced SMAP SM [46, 58, 59]. Basic information of the above-mentioned satellite-based SM, including names, spatial resolutions, temporal resolutions, and abbreviations, are listed in Table I.

TABLE I. BASIC INFORMATION OF SATELLITE-BASED SM PRODUCTS

Name	Spatial resolution	Temporal resolution	Abbreviation
ECV Passive Combined SM	0.25°	Daily	ECV_P
ECV Active and Passive Combined SM			ECV_C
SMAP Ascending SM	9 km		SMAP_A_9
SMAP Descending SM			SMAP_D_9
SMAP Ascending SM	36 km		SMAP_A_36
SMAP Descending SM			SMAP_D_36

B. IN-SITU MEASUREMENTS

Eight in-situ networks in Europe are applied in this study (Figure 1). All the in-situ data are acquired from the International Soil Moisture Network (https://ismn.geo.tuwien.ac.at/en/) [60]. Each of them has been utilized for SM evaluation, calibration, and uncertainty analysis in previous studies, and has revealed consistent performance [61-68]. Basic attributes of each in-situ measurement are listed in Table II. It can be seen that these in-situ measurements are located in regions with abundant climate types and biomes that could be employed to carry out systematical and comprehensive validation process. The topsoil humidity records at 5 cm depth are chosen to validate performances of the remotely sensed SM products. Additionally, to maintain the stability of the data series, daily in-situ SM is calculated from the arithmetic mean of hourly-monitored value.

TABLE II. BASIC ATTRIBUTES OF THE EIGHT IN-SITU MEASUREMENTS

| Name	Nation	Station Number	Region Climate	Land Cover Types	Reference
REMEDHUS	Spain	20	temperate marine climate	cropland and Shrubland	Sanchez et al. [61]
FR_Aqui	France	4	Mediterranean climate	cropland and forest	Albergel et al. [62]
FMI	Sweden	20	climate of sub-frigid coniferous forest	woody savanna	Zeng et al. [63]
HOBE	Denmark	27	temperate marine climate	cropland and forest	Jensen et al. [64]
BIEBRZA_S	Poland	18	temperate continental climate	grassland and marshland	Katarzyna et al. [65]
TERENO	Germany	5	temperate marine climate	cropland and forest	Bogena et al. [66]
RMSN	Romania	19	temperate continental climate	cropland and forest	Sandric et al. [67]
SMOSMANIA	France	21	Mediterranean climate	diverse land cover	Calvet et al. [68]
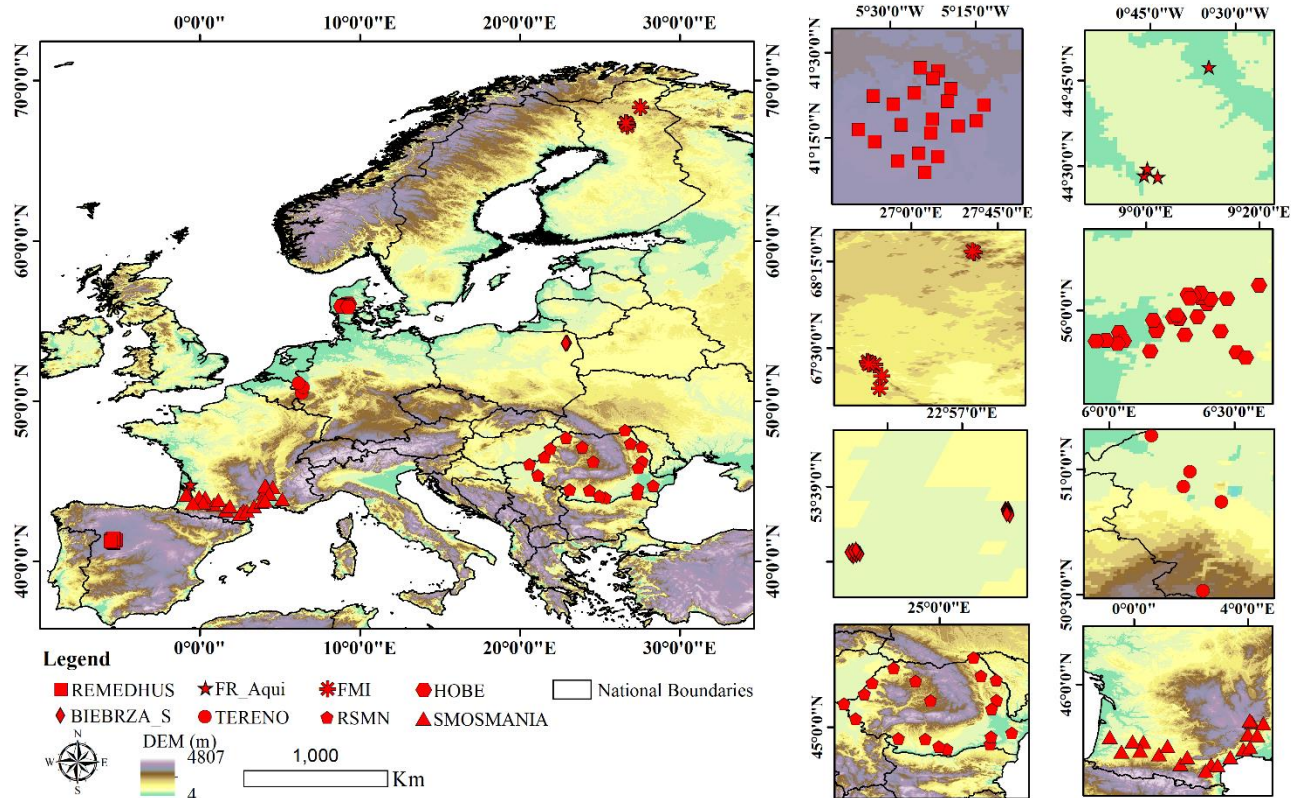
FIGURE 1. Distribution of the eight in-situ networks in Europe

C. GAP-FILLING METHOD

Firstly, the accuracy of the original ECV and SMAP SM products are compared to clarify their initial quality levels under diverse in-situ measurements and to discuss the potential of SMAP in filling the gaps of ECV. In particular, the correlation coefficient (CC), bias, and unbiased root mean square error (ubRMSE) are selected as error parameters to objectively and systematically depict data accuracy. CC is a statistical index firstly designed by statistician Carl Pearson [69]. It is an indicator that could be used to analyze the linear correlation degree of two variables. Bias reflects the error between the output of the regression model based on the sample and the true value, that is, the accuracy of the model itself [70]. According to the positive and negative values, it can be divided into overestimation and underestimation, respectively. UbRMSE depicts the difference in dispersion between satellite-based SM values and corresponding in-situ measurements [71]. Additionally, defined by the SMOS and SMAP community, satellite retrieved SM are expected to get a target accuracy of ubRMSE ≤ 0.04 m³/m³ [32, 46]. Therefore, these metrics allow us to objectively explore the accuracy of SMAP and ECV SM datasets over the case study areas. And their equations are listed as follows.

$$CC = \frac{\sum_{i=1}^{n}(Y_i - \bar{Y})(X_i - \bar{X})}{\sqrt{\sum_{i=1}^{n}(Y_i - \bar{Y})^2}\sqrt{\sum_{i=1}^{n}(X_i - \bar{X})^2}} \quad (2)$$

$$Bias = \frac{\sum_{i=1}^{n}X_i - \sum_{i=1}^{n}Y_i}{n} \quad (3)$$

$$ubRMSE = \sqrt{\frac{\sum_{i=1}^{n}[(X_i - \bar{X}) - (Y_i - \bar{Y})]^2}{n}} \quad (4)$$

where X_i, $\bar{X}$, Y_i, $\bar{Y}$ are remotely sensed SM value at pixel i, arithmetic means of all remotely sensed SM pixels, in-situ measurements value at station i, and averaged value of all in-situ measurements values, respectively.

Then, the 9 km and 36 km SMAP are resampled to 0.25° spatial resolution (to maintain accordance with the spatial resolution of ECV) by calculating their arithmetic means, and taken to fill the null value region of ECV SM. The global spatial null value percent of the original ECV and gap-filled ECV SM products from 1st January 2016 to 31st December 2017 are illustrated to explore their initial spatio-temporal coverage integrity and analyze the space integrity improvement after gap-filling process. Additionally, for quantitative evaluation, CC, bias, and ubRMSE are together utilized to explain the fitting degree and accuracy of different gap-filled results. Meanwhile, the probability density function (PDF) curves [72] are drawn to analyze the SM value distribution features of each gap-filled SM product and in-situ measurements, trying to figure out the rectification degree of value distribution after the gap-filling procedure. Moreover, the time series evolution curves are drawn to reveal temporal goodness of fit between gap-filled ECV SM products and in-situ measurements.

III. RESULTS

A. ACCURACY ANALYSIS OF THE ORIGINAL SATELLITE RETRIEVED SM PRODUCTS

Figures 2-4 display boxplots of CC, bias, and ubRMSE among the eight in-situ measurements. The horizontal lines from top to bottom in boxplots can effectively show the upper edge, upper four quantile, median, lower four quantile, lower edge, and outliers (red points) of an array [73]. There are significant differences among the multiple sensor-derived SM products in in-situ measurements validation results. Comparatively speaking, the ECV_C, synthesized by ECV_A and ECV_P, shows a generally better accuracy than ECV_P both in fitting degree and in value errors. In comparison, SMAP-derived SM datasets achieve outstanding performance among the assessed products. They even remarkably surpass ECV_C in terms of CC as shown in Figure 2 (c), (f), (g), and (h), and in terms of bias in Figure 3 (a), (b), and (h). It seems that spatial resolution may not be the main factor affecting accuracy, as at both 9 km and 36 km pixel resolution SMAP SM are verified to have high accuracy to in-situ measurements. The ascending SMAP has slightly better ability in representing all-day surface SM than the corresponding descent acquisition occurring in the night when there is dew [65]. The overall performances of CC, bias, and ubRMSE co-confirm the prominence of SMAP-retrieved SM, namely, the distinguished SM depicting capability of the L-band centered at 1.41 GHz. Summarily, the SMAP SM products could be qualified candidates for ECV to adopt to further enhance data integrity and quality.

Considering different in-situ networks, the validation results of REMEDHUS, TERENO, and SMOSMANIA are favorable. Both ECV and SMAP products could precisely match the dynamics and values of in-situ measurements with average CC higher than 0.7 and bias close to 0. Nevertheless, the original SM products does not accurately match the in-situ measurements in the FMI and BIEBRZA_S-1 networks, accompanied by relatively obvious errors. At the FMI network, although the SMAP products outperform ECV products with good data accuracy, SMAP always significantly overestimates the in-situ measurements, shown by Figure 3 (c). This phenomenon may be associated with its cold climate, as recent studies conducted in the Tibetan Plateau, which locates in cold climate region, also display unfavorable performance of satellite retrieved SM products [7, 63]. The BIEBRZA_S-1 network is located in wetland ecosystems, where SM values are several times higher than in agricultural areas. According to a recently research in BIEBRZA_S-1 network, the SM products retrieved from Sentinel-1 express a CC value of approximate 0.5 at 5 cm depth, which is essentially in agreement with the outcome in our study [65].
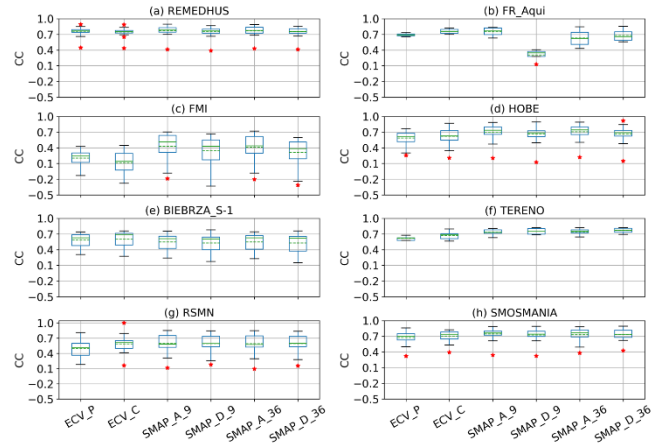

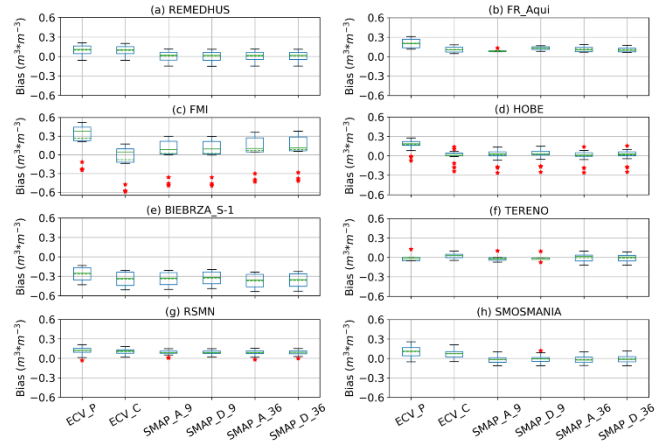**Figure 2.** Boxplot of CC among eight in-situ measurements

Figure 3. Boxplot of bias among eight in-situ measurements

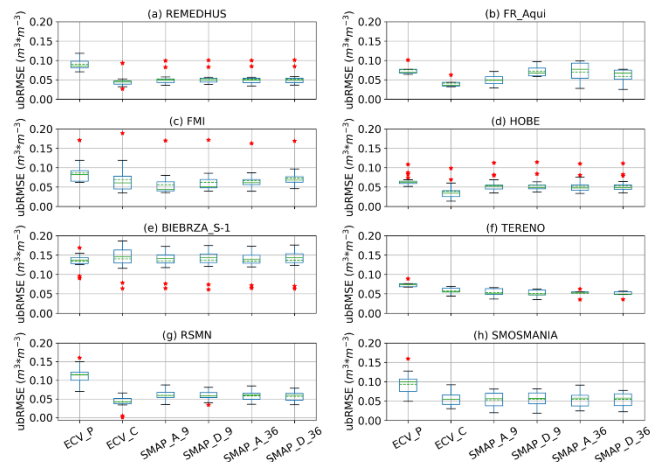**Figure 4.** Boxplot of ubRMSE among eight in-situ measurements

## B. SPATIAL COVERAGE INTEGRITY PERFORMANCES

Although ECV has already developed a global scale SM product with 40-year time series, the limited spatial coverage percent remains a challenge that notably restricts its spatio-temporal consistency. The missing data could be inevitably induced by regular relative motion between the satellite and

Earth. Meanwhile, both radio-frequency interference (RFI) and dense vegetation could introduce microwave echo signal gaps [74]. Figures 2 shows the data missing percentages of the original and gap-filled ECV SM from 1st January 2016 to 31st December 2017, respectively. Essentially, active and passive SM products combined ECV_C datasets (Figure 2(b)) achieves relatively low missing percentages. They obtained less than 40% missing data at the middle and low latitude zones, while the missing percentages could achieve 60-80% at 60-90°N. Instead, the ECV_P (Figure 2(a)) displays much larger missing day percentages. Specifically, the space integrity improvement of ECV_P could be in urgent need.

In comparison, after the gap-filling process, the days missing percent of both ECV_P and ECV_C are evidently decreased. As shown in Figure 5 (c)-(j), the high missing percentage areas in Figure 5 (a)-(b), such as the Qinghai-Tibet Plateau, the Central Siberian Plateau, and the Rocky Mountains, all improve their coverage percentages from about 20-40% to 40-60%. Additionally, in Northern South America and Central Africa, where the Amazon Rain Forest and the Sahara Desert situated in, the days missing percentages obviously shrink from 100% to 40-60%. Besides, this paper displays the original and the gap-filled results in 1st July 2016 and 1st July 2017 in Europe (as shown in Figure 6). The null value region could be effectively and smoothly filled by SMAP SM products after resample. In particular, at high latitudes, the ECV_P significantly overestimate the FMI in-situ measurements, however, the overestimation level in the gap region filled by SMAP can be reduced significantly. As a result, the SMAP SM products reveal its capability both in filling the gap and in improving the accuracy of the original ECV_P SM.
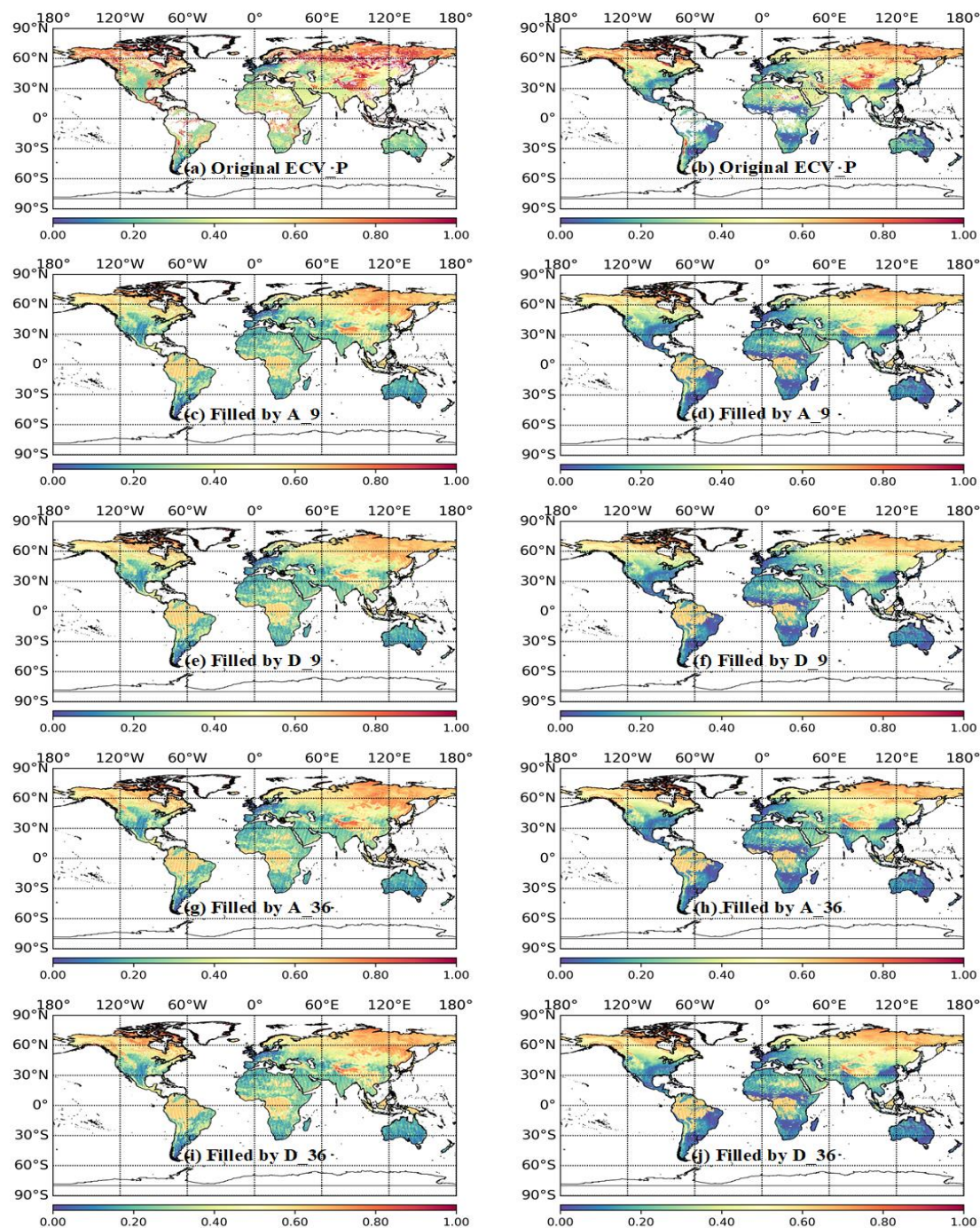
Figure 5. Days missing percent of the original and gap-filled ECV_P and ECV_C SM data using different SMAP SM products. (Unit: ×100%)
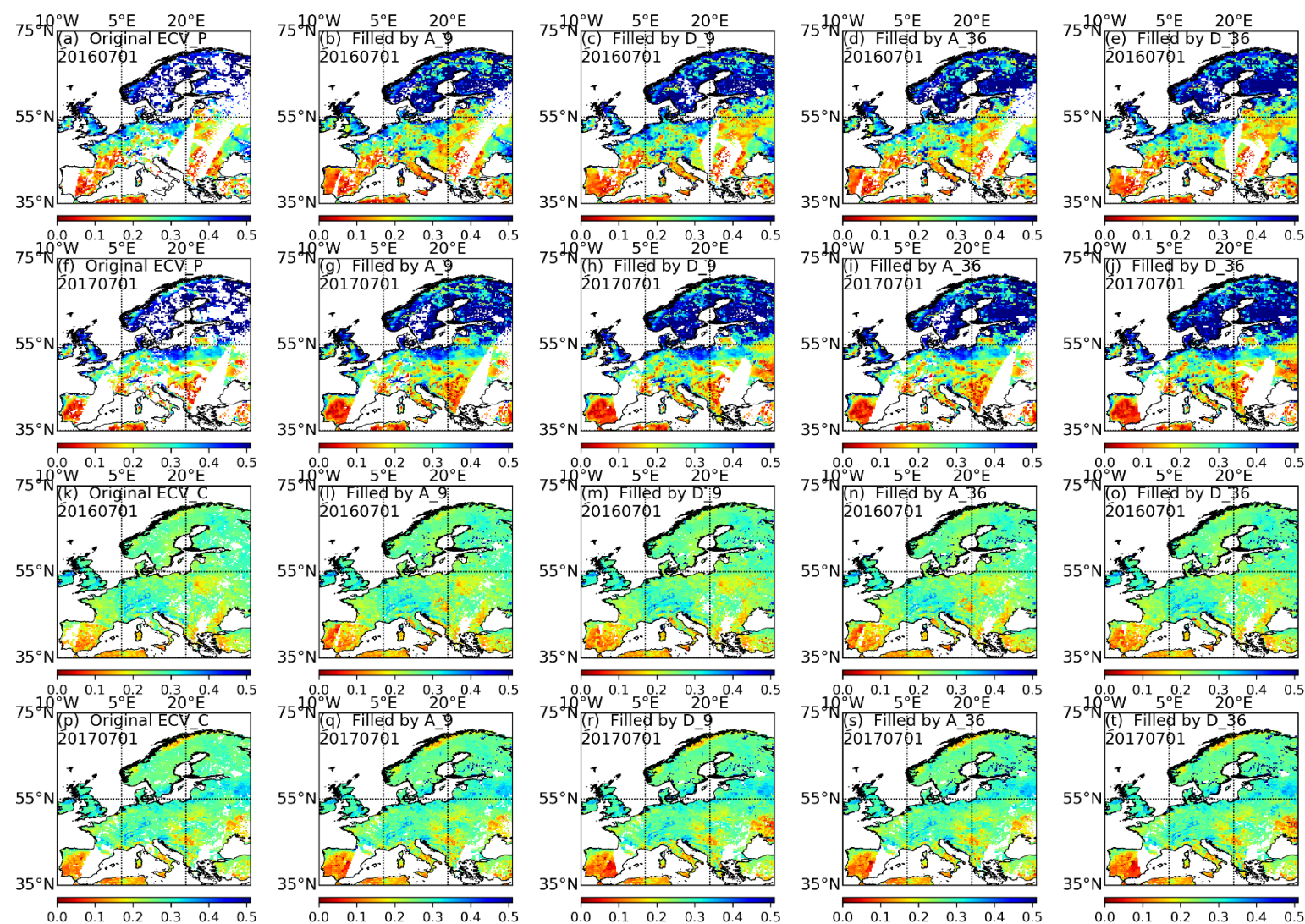
Figure 6. Original ECV SM products and corresponding gap-filled results using different SMAP SM products in 1st July 2016 and 1st July 2017. (Unit: m^3×m^{-3})

C. COMPARISON OF THE ORIGINAL AND GAP-FILLED ECV SM

1) ACCURACY ANALYSIS

Given the good performances of SMAP retrieved SM products in precisely representing the dynamic feature and value of the in-situ measurements, they are taken to fill the gaps of the ECV SM in this study. The 9 km and 36 km SMAP SM products (including ascending and descending ones) are resampled to the resolution of 0.25° grid to keep in line with ECV. The blank regions in ECV SM are filled by different SMAP products, and the accuracy of the gap-filled results among the eight in-situ measurements are displayed in Table III. Since the accuracy results are relative analogous to each

other, we employ table instead of boxplot to illustrate their values.

Table III shows the comparison of the accuracy of the original and gap-filled ECV SM products. It can be clearly seen that ECV products filled by upscaled 9 km SMAP and downscaled 36 km SMAP achieve similar good response to the in-situ measurements. Meanwhile, the gap-filled results by ascending and descending SMAP express quite similar performance to each other. In particular, the accuracy of ECV_P in REMEDHUS in-situ measurements is excellent. At the REMEDHUS network, compared to the original ECV_P, the CC and bias in gap-filled ECV_P can be effectively enhanced and decreased, respectively. Both integrity and accuracy can be significantly improved in this network.

TABLE III. ACCURACY OF THE ORIGINAL AND GAP-FILLED ECV SM PRODUCTS. A_9, D_9, A_36, D_36 REFER TO ECV SM PRODUCTS FILLED BY SMAP_A_9, SMAP_D_9, SMAP_A_36, SMAP_D_36, RESPECTIVELY

In-situ Measurements		ECV_P					ECV_C				
		Original	A_9	D_9	A_36	D_36	Original	A_9	D_9	A_36	D_36
REMEDHUS	CC	0.76	0.81	0.81	0.81	0.81	0.75	0.74	0.75	0.74	0.75
	Bias	0.10	0.08	0.08	0.08	0.08	0.09	0.07	0.08	0.07	0.08
	ubRMSE	0.09	0.09	0.08	0.09	0.08	0.05	0.05	0.05	0.05	0.05
FR_Aqui	CC	0.69	0.67	0.68	0.68	0.68	0.76	0.76	0.77	0.76	0.76
	Bias	0.21	0.17	0.17	0.17	0.17	0.11	0.11	0.11	0.11	0.11
	ubRMSE	0.08	0.08	0.08	0.08	0.08	0.04	0.04	0.04	0.04	0.04
FMI	CC	0.20	0.13	0.13	0.15	0.15	0.11	0.21	0.21	0.19	0.19
	Bias	0.27	0.17	0.18	0.20	0.21	-0.08	-0.01	-0.01	-0.01	-0.01
	ubRMSE	0.09	0.15	0.15	0.13	0.13	0.07	0.05	0.05	0.06	0.06
HOBE	CC	0.59	0.49	0.50	0.49	0.51	0.62	0.55	0.53	0.53	0.52
	Bias	0.17	0.16	0.16	0.16	0.16	0.00	-0.01	0.00	-0.01	0.00
	ubRMSE	0.07	0.07	0.07	0.07	0.07	0.04	0.05	0.05	0.05	0.05
BIEBRZA_S-1	CC	0.59	0.67	0.67	0.65	0.65	0.60	0.57	0.59	0.58	0.60
	Bias	-0.27	-0.27	-0.27	-0.28	-0.28	-0.34	-0.34	-0.34	-0.35	-0.35
	ubRMSE	0.13	0.11	0.11	0.11	0.11	0.14	0.13	0.13	0.13	0.13
TERENO	CC	0.62	0.64	0.65	0.65	0.65	0.67	0.55	0.56	0.66	0.71
	Bias	0.00	-0.02	-0.02	-0.01	-0.01	0.02	0.03	0.03	0.03	0.03
	ubRMSE	0.08	0.07	0.07	0.07	0.07	0.06	0.06	0.06	0.05	0.05
RSMN	CC	0.50	0.49	0.49	0.49	0.49	0.56	0.56	0.56	0.56	0.56
	Bias	0.12	0.11	0.11	0.11	0.11	0.11	0.10	0.10	0.10	0.10
	ubRMSE	0.12	0.11	0.11	0.11	0.11	0.05	0.05	0.05	0.05	0.05
SMOSMANIA	CC	0.67	0.64	0.61	0.61	0.62	0.62	0.70	0.63	0.63	0.63
	Bias	0.10	0.07	0.08	0.08	0.08	0.08	0.07	0.07	0.07	0.07
	ubRMSE	0.09	0.06	0.10	0.10	0.10	0.10	0.06	0.06	0.06	0.06

*Unit of bias and ubRMSE is $m^3 \times m^{-3}$

2) PDF DISTRIBUTION

PDF curves among the eight in-situ networks are drawn to tentatively explore the value distribution characteristics of each kind of SM product (Figure 7) [72]. Comparatively, the PDF of in-situ measurements obtain lower maximum probability percentages than satellite-based SM products; in other words, the in-situ measurements generally have more decentralized distribution of SM values than remotely sensed SM. Actually, the ground sensors could monitor SM on hourly or sub-hourly scale, and the daily SM value is acquired

through calculating their arithmetic mean. Hence, the daily SM value from in-situ measurements can represent the average SM condition of a whole day. In comparison, because of the instantaneous transit of satellites, the satellite retrieved data could only record the SM at a certain time point within a day. It is suggested that the different measurement frequencies could be a reason that result to the heterogeneity of PDF shapes.

Compared to ECV_C, the shapes of original ECV_P and its gap-filled results display more analogous PDF shapes to the

in-situ measurements in the TERENO and SMOSMANIA networks, as shown in Figure 7(f) and (h). It is worth mentioning that although the ECV_C shows favorable accuracy, which is proved in the first part of section IV, its maximum probability percent is much higher than the ECV_P and the in-situ measurements in Figure 7 (c)-(f).

In terms of the gap-filled results, it could be preliminarily inferred that even though there are remarkable spatial resolution differences between the 9 km and 36 km SMAP products, their gap filling results express similar performance. And the difference between ECV SM products filled by ascending and descending SMAP SM products is not obvious.

Besides, the gap-filled results have an advantage in balancing the SM value distribution percentage of the original ECV SM products, especially the ECV_C SM. For instance, as shown in Figure 7 (a), (c), (d), (e), and (f), the maximum probability percentages of gap-filled ECV_C results are evidently decreased, and the corresponding SM values get closer to the in-situ measurements than the original ECV_C ones. Consequently, this rectification result suggests that the SMAP has competent potential in improving the spatial coverage percent and enhancing the data accuracy of the original ECV SM products.
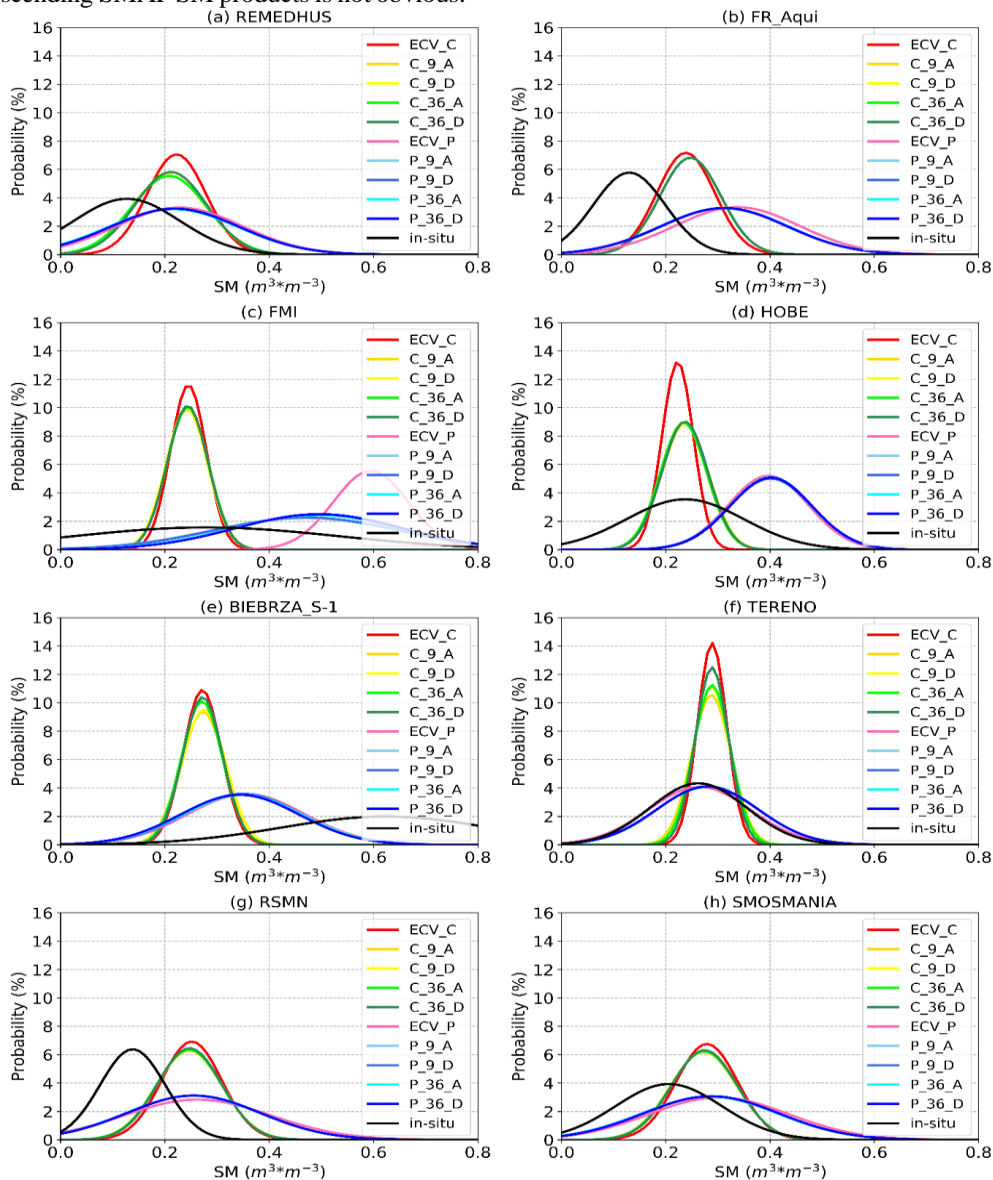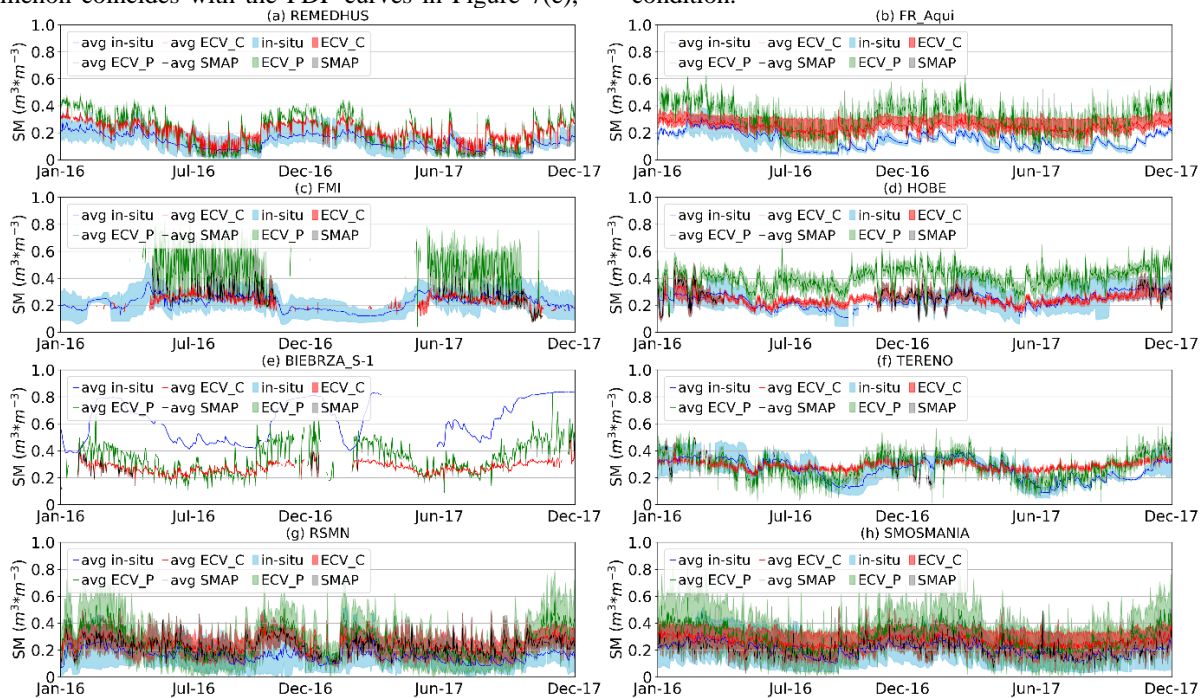

Figure 7. SM PDF curves in different in-situ measurements: (a) REMEDHUS, (b) FR_Aqui, (c) FMI, (d) HOBE, (e) BIEBRZA_S-1, (f) TERENO, (g) RSMN, and (h) SMOSMANIA. C_A_9, C_D_9, C_A_36, C_D_36 refer to ECV_C SM products filled by SMAP_A_9, SMAP_D_9, SMAP_A_36, SMAP_D_36, respectively. P_A_9, P_D_9, P_A_36, P_D_36 refer to ECV_P SM products filled by SMAP_A_9, SMAP_D_9, SMAP_A_36, SMAP_D_36, respectively.

3) TEMPORAL EVOLUTION TRENDS

Temporal evolution tendency could efficiently depict annual variation of different SM products. The SM fluctuation curves from 1st January 2016 to 31st December 2017 are drawn in Figure 8 to systematically compare the fitting degree between gap-filled ECV_C, ECV_P and the in-situ measurements. The red lines, indicating gap-filled ECV_C, achieve good accordance to the in-situ measurements. In comparison, the gap-filled ECV_P (green lines) displays relative obvious overestimation in the FMI and HOBE networks, as shown in Figure 8(c) and (d). However, both ECV_C and ECV_P evidently underestimate the in-situ measurements in BIEBRZA_S-1 (Figure 8 (e)). This phenomenon coincides with the PDF curves in Figure 7(e),

where the value ranges of in-situ measurements sparsely distribute in 0.5-0.8 $m^3 \times m^{-3}$. Actually, hybrid pixels in this region are composed by marshland as well as grassland, leading to wet condition all year round [65]. It could be implied that the accuracy of remotely sensed microwave SM in wetland area needs further improvement. Moreover, the SMAP products, which participate in the gap-fill process, are also displayed in Figure 8 through black lines. It can be seen that, compared to multi passive bands retrieved ECV_P, the L-band derived SMAP could accurately fit the temporal evolution trend of in-situ measurements, further proving its outstanding performance in representing surface SM condition.

Figure 8. SM time-series evolution in different in-situ measurements from 1st January 2016 to 31st December 2017: (a) REMEDHUS, (b) FR_Aqui, (c) FMI, (d) HOBE, (e) BIEBRZA_S-1, (f) TERENO, (g) RSMN, and (h) SMOSMANIA.

IV. DISCUSSION

Satellite-retrieved SM has been broadly utilized in global climate change, surface hydrological cycle, agricultural water management, and other relative fields [3, 5, 75]. The multi-sensor based ECV SM has attracted widespread attentions and thorough studies since its inception, whereas frequent null value regions and limited data accuracy hinder its integrity and in-depth application. Hence, this research attempts to explore the potential of SMAP SM products in filling the gaps of ECV SM, so as to undertake additional efforts to improve the quality of ECV SM.

A. PARAMETER ANALYSIS OF SATELLITE-BORNE SENSORS

The ECV dataset is originated from the integration of diverse active passive sensor-based SM products. The basic information of each sensor is listed in Table IV. The time ranges in Table IV reveal that every SM product has its own time series duration. For example, SSM/I, launched in 1987,

is still in service. By contrast, AMSR-E has already completed its nine-year mission from 2002 to 2011. Furthermore, the upcoming ECV SM with continuous time series update would come from the fusion of the ongoing MetOp-A ASCAT, MetOp-B ASCAT, SSM/I, AMSR-2, Windsat, and SMOS. Therefore, it is necessary to steadily develop and add new SM products to prolong ECV SM. In this study, it is preliminarily proved that the SMAP SM could be conducive to enhancing the spatial integrity and quality of ECV SM.

As a newly emerging satellite-based SM products with long service lives, SMAP might have a promising potential in assuring temporal coherence and continuity of ECV SM. Moreover, compared to the other ongoing sensors, the SMAP has unique ascending and descending time nodes, which could also be helpful in enriching daily SM information with enhanced data stability and superior representation levels.

TABLE IV. BASIC ATTRIBUTES OF ECV AND SMAP SENSORS

SM Products	Time ranges	Ascending/ Descending Time Nodes	Sensor Types	Bands	Penetration Depths	Spatial Resolutions	Temporal Resolutions
ERS-1	1991.7.17-2000.3.10	22:15 (A), 10:30 (D)	scatterometer	C-band (5.3GHz)	< 2 cm	50 ×50 km	
ERS-2	1995.4.21-2011.9.5	22:30 (A), 10:30 (D)	scatterometer	C-band (5.3GHz)	< 2 cm	25 ×25 km^2	
MetOp-A ASCAT	2006.10.19 on going	21:30 (A), 09:30 (D)	scatterometer	C-band (5.3GHz)	< 2 cm	25×25 km^2	
MetOp-B ASCAT	2012.9.17 on going	21:30 (A), 09:30 (D)	scatterometer	C-band (5.3GHz)	< 2 cm	25×25 km^2	
SMMR	1979-1987	12:00 (A), 24:00 (D)	radiometer	C-band (6.6 GHz), Ka-band (37 GHz)	< 2 cm	150×150 km^2	
SSM/I	1987 on going	DMSP-F08 06:12 (A), 18:12 (D) DMSP-F11 18:11 (A), 06:11 (D) DMSP-F13 17:42 (A), 05:42 (D)	radiometer	K-band (19.4 GHz), Ka-band (37.0 GHz)	< 1.5 cm	69×43 km^2	daily
TMI	1997.12.7-2015.4.8	changes 24 hours of local time in 46-day procession	radiometer	X-band (10.65 GHz), Ka-band (37.0 GHz)	< 3 cm	59×36 km^2	
AMSR-E	2002.6.1-2011.10.4	01:30 (A), 13:30 (D)	radiometer	C-band (6.9 GHz), X-band (10.7 GHz)	< 2 cm	76×44 km^2	
AMSR-2	2012.8.10 on going	01:30 (A), 13:30 (D)	radiometer	C-band (6.9 GHz), X-band (10.7 GHz)	< 2 cm	35×62 km^2	
Windsat	2003.2.13 on going	18:10 (A), 06:10 (D)	radiometer	C-band (6.8 GHz)	< 2 cm	25×35 km^2	
SMOS	2009.11.2 on going	06:00 (A), 18:00 (D)	radiometer	L-band (1.4 GHz),	~ 5 cm	40×40 km^2	
SMAP	2015.1.31 on going	18:00 (A), 06:00 (D)	scatterometer radiometer	L-band (1.4 GHz)	~ 5 cm	3×3/9×9/36×36 km^2	

IEEE *Access*
Multidisciplinary : Rapid Review : Open Access Journal

B. IMPROVING SPATIAL COVERAGE, DATA COVERAGE, AND VALUE DISTRIBUTION

In this study, the spatial coverage percentage of ECV SM is analyzed to illustrate the necessity of enhancing its land coverage integrity. Although composed by multiple satellite-retrieved SM products, the gap regions of ECV SM, mainly caused by the RFI, dense vegetation, and satellite scanning gaps, can be seen everywhere. Therefore, it is beneficial for SMAP to fill the gaps of ECV SM products and increase spatial coverage integrity. Meanwhile, the accuracy of the original SMAP and ECV SM products are evaluated against eight in-situ measurements in Europe with diverse hydrothermal combination conditions and underlying surface types. The L-band derived SMAP SM (including ascending and descending products on 9 km and 36 km scales) could outperform multi bands fused ECV SM in both fitting degree and value errors.

Detailed analysis is processed by comparisons between the gap-filled ECV and original ECV to discuss the improvement after the participation of SMAP. First of all, the data coverage ratio of gap-filled ECV increases 20% on average. The improved spatial integrity coverage can effectively promote studies focused on regional daily continuous SM evolution analysis. Secondly, the accuracy is objectively and systematically evaluated by using in-situ measurements. Results illustrate that compared to the original ECV, the gap-filled ECV products express similar good response to the in-situ measurements, suggesting that the SMAP SM products could consistently maintain favorable accuracy even after spatial resample. In particular, the gap-filled results get better accuracy than the original ECV in REMEDHUS network. Thirdly, in terms of SM value distribution, the original ECV_C prominently demonstrates extremely high maximum percentages reflected by PDF curves, revealing remarkably concentrated SM values. Although previous studies have stated the superiority of ECV_C [34, 35], it seems that the over-centralized value distribution may be a restriction that limits accuracy improvement. Fortunately, this eminent drawback could be effectively rectified through gap-filling progress using SMAP.

In this study, the accuracy evaluation results indicate that SMAP soil moisture gets superior precision than ECV soil moisture over most networks. Therefore, it seems that it may be more valuable to formulate a seamless SMAP soil moisture dataset through filling its gaps using ECV. However, it was not until 2015 that the SMAP program was initiated, which means that the its time span could be obviously shorter than the 40-year time series ECV soil moisture dataset. We think that it could be more beneficial to analyzing climate evolution trends using a good soil moisture dataset with decades of time series. Additionally, with the development of artificial intelligence technology, previous studies have proved that the gaps of SMAP could be effectively filled by machine learning algorithms [76, 77].

C. THE ADVANTAGES OF L-BAND IN SM RETRIEVAL

This study explores the applicability of SMAP in enhancing the space coverage integrity of ECV SM and finds that the L-band retrieved SMAP SM could reveal remarkable advantages. The L-band radiometer has revealed exceptional capability in acquiring high accuracy SM since inception [15, 37, 63, 78]. Both SMOS and SMAP soil moisture are retrieved from L-band signals. The SMOS could be a forerunner of L-band retrieved global soil moisture with a ground resolution of 50 km [32]. It firstly uses a single-orbit and then upgrades to a multi-orbit retrieval algorithm to derive soil moisture. The SMAP retrieved 36-km grid soil moisture from L-band radiometer is based on inversion of the tau–omega model which includes features to mitigate the disturbances from RFI [79]. To protect the L-band from unexpected illegal RFI, it is prohibited by international agreements at the observation band of the SMAP radiometer (1.4-1.427 GHz) [80]. However, since the L-band signals are vulnerable to illegal RFI, the accuracy of SMOS retrieved soil moisture can be disturbed by both large-level and low-level interferences. In comparison, the SMAP program takes various measures to avoid RFI as much as possible. It incorporates aggressive RFI avoidance and filtering for the radiometer. Ground RFI detectors and almost 1000 times more measurements than previously used are jointly applied to remove multiple interferences [81]. With these safeguard measures simultaneously, SMAP can successfully develop high accuracy SM products and keep optimizing the performance of the sensor and corresponding products.

In addition, currently most on-board microwave sensors adopt C, K, Ka, and X bands to acquire the top 2 cm SM. Comparatively, SMAP utilizes the L-band to calculate SM at approximate 5 cm depth; which means that, after the participation of SMAP, ECV SM may obtain richer band information and closer depth matching to ground stations than before. Because the in-situ measurements usually monitor top layer soil humidity hourly with water probes at 5 cm depth, it is suggested that ECV SM may gain more consistent depth matching to the ground stations by absorbing the L-band SMAP SM.

V. CONCLUSION

As a multiple satellite-derived active and passive sensor merged SM product, ECV SM has received extensive attention because of its global coverage, and superior data accuracy compared to its constituent components. For the sake of continuously reducing the null value region and enhancing data accuracy, this study explores the potential applicability of SMAP in filling the gaps of ECV SM through a case study in Europe.

The validation outcomes indicate that no matter upscaling or downscaling, the resampled SMAP could efficiently fill the gaps of ECV SM with satisfying accuracy. Meanwhile, both ascending and descending SMAP products behave good performances, testifying the robustness of L-band retrieved

SM products. Furthermore, it may be feasible to integrate the ascending and descending SMAP into one day-scale SM product, which could be used to further enhance the spatial integrity of SM with favorable accuracy. On the whole, this study conducts objective and detailed evaluation on the performance of applying SMAP to improve the spatial completeness of ECV, and is expected to act as a valuable reference in ECV SM gap-filling method. In addition, it is found that the underestimation of on-board sensors retrieved SM in marshland can be very large, which means there is a long way to go to steadily improve the on-board microwave sensitivity in humid regions such as wetland.

In this study, we attempt to take SMAP to enhance the integrity of ECV SM, and achieve positive conclusions. However, much work needs to be done to further promote the process. It is noticed that although the spatial coverage percent can be significantly improved after the gap-filling, there still has sparsely distributed null value regions. It is recommended that more satellite retrieved SM products with excellent accuracy, long time series, and global coverage could be taken to improve the ECV SM and gradually generate a global land surface seamlessly covered SM product.

ACKNOWLEDGMENT

REFERENCES

[1] R. Bindlish et al., "GCOM-W AMSR2 Soil Moisture Product Validation Using Core Validation Sites," IEEE Journal of Selected Topics in Applied Earth Observations & Remote Sensing, vol. 11, no. 1, pp. 209-219, 2018.

[2] A. Al Bitar et al., "Evaluation of SMOS soil moisture products over continental US using the SCAN/SNOTEL network," IEEE Transactions on Geoscience and Remote Sensing, vol. 50, no. 5, pp. 1572-1586, 2012.

[3] R. Bindlish et al., "Soil moisture estimates from TRMM Microwave Imager observations over the Southern United States," Remote Sensing of Environment, vol. 85, no. 4, pp. 507-515, 2003.

[4] Y. Liu, Y. Yang, and X. Yue, "Evaluation of Satellite-Based Soil Moisture Products over Four Different Continental In-Situ Measurements," Remote Sensing, vol. 10, no. 7, p. 1161, 2018, doi: 10.3390/rs10071161.

[5] K. Fan et al., "Spatiotemporal impact of soil moisture on air temperature across the Tibet Plateau," Science of the Total Environment, vol. 649, pp. 1338-1348, 2019.

[6] J. Im, S. Park, J. Rhee, J. Baik, and M. Choi, "Downscaling of AMSR-E soil moisture with MODIS products using machine learning approaches," Environmental Earth Sciences, vol. 75, no. 15, 2016, doi: 10.1007/s12665-016-5917-6.

[7] J. Zeng, Z. Li, Q. Chen, H. Bi, J. Qiu, and P. Zou, "Evaluation of remotely sensed and reanalysis soil moisture products over the Tibetan Plateau using in-situ observations," Remote Sensing of Environment, vol. 163, pp. 91-110, 2015, doi: 10.1016/j.rse.2015.03.008.

[8] W. A. Dorigo et al., "Error characterisation of global active and passive microwave soil moisture datasets," Hydrology and Earth System Sciences, vol. 14, no. 12, pp. 2605-2616, 2010, doi: 10.5194/hess-14-2605-2010.

[9] R. H. Reichle, R. D. Koster, J. Dong, and A. A. Berg, "Global Soil Moisture from Satellite Observations, Land Surface Models, and Ground Data: Implications for Data Assimilation," Journal of Hydrometeorology, vol. 5, no. 3, p. 2004, 2009.

[10] B. W. Barrett, E. Dwyer, and P. Whelan, "Soil moisture retrieval from active spaceborne microwave observations: An evaluation of current techniques," Remote sensing, vol. 1, no. 3, pp. 210-242, 2009.

[11] H. Su, B. Yong, and Q. Du, "Hyperspectral Band Selection Using Improved Firefly Algorithm," IEEE Geoscience and Remote Sensing Letters, vol. 13, no. 1, pp. 68-72, 2016, doi: 10.1109/LGRS.2015.2497085.

[12] H. Su, B. Zhao, Q. Du, and P. Du, "Kernel Collaborative Representation With Local Correlation Features for Hyperspectral Image Classification," IEEE Transactions on Geoscience and Remote Sensing, vol. 57, no. 2, pp. 1230-1241, 2019, doi: 10.1109/TGRS.2018.2866190.

[13] H. Su, B. Zhao, Q. Du, P. Du, and Z. Xue, "Multifeature Dictionary Learning for Collaborative Representation Classification of Hyperspectral Imagery," IEEE Transactions on Geoscience and Remote Sensing, vol. 56, no. 4, pp. 2467-2484, 2018, doi: 10.1109/TGRS.2017.2781805.

[14] J. Peng, A. Loew, S. Zhang, J. Wang, and J. Niesel, "Spatial downscaling of satellite soil moisture data using a vegetation temperature condition index," IEEE Transactions on Geoscience and Remote Sensing, vol. 54, no. 1, pp. 558-566, 2016.

[15] M. S. Burgin et al., "A Comparative Study of the SMAP Passive Soil Moisture Product With Existing Satellite-Based Soil Moisture Products," IEEE Transactions on Geoscience & Remote Sensing, vol. 55, no. 5, pp. 2959-2971, 2017.

[16] T. Lacava et al., "A multi-sensor (SMOS, AMSR-E and ASCAT) satellite-based soil moisture products inter-comparison," in Geoscience & Remote Sensing Symposium, 2012.

[17] C. D. O. A. Filho and D. D. F. Rossetti, "Effectiveness of SRTM and ALOS-PALSAR data for identifying morphostructural lineaments in northeastern Brazil," International Journal of Remote Sensing, vol. 33, no. 4, pp. 1058-1077, 2012.

[18] V. Kerbaol, B. Chapron, and P. W. Vachon, "Analysis of ERS-1/2 synthetic aperture radar wave mode imagettes," Journal of Geophysical Research Oceans, vol. 103, no. C4, pp. 7833-7846, 1998.

[19] R. Torres et al., "GMES Sentinel-1 mission," Remote Sensing of Environment, vol. 120, pp. 9-24, 2012.

[20] E. G. Njoku, T. J. Jackson, V. Lakshmi, T. K. Chan, and S. V. Nghiem, "Soil moisture retrieval from AMSR-E," IEEE Transactions on Geoscience & Remote Sensing, vol. 41, no. 2, pp. 215-229, 2003.

[21] R. M. Parinussa, T. R. H. Holmes, N. Wanders, W. A. Dorigo, and R. A. M. De Jeu, "A Preliminary Study toward Consistent Soil Moisture from AMSR2," Journal of Hydrometeorology, vol. 16, no. 2, pp. 932-947, 2013.

[22] Jackson et al., "Validation of Soil Moisture and Ocean Salinity (SMOS) Soil Moisture Over Watershed Networks in the U.S,"

IEEE Transactions on Geoscience & Remote Sensing, vol. 50, no. 5, pp. 1530-1543, 2012.

[23] W. Dorigo *et al.*, "ESA CCI Soil Moisture for improved Earth system understanding: State-of-the art and future directions," *Remote Sensing of Environment,* vol. 203, 2017.

[24] N. Pan, S. Wang, Y. Liu, W. Zhao, and B. Fu, "Global Surface Soil Moisture Dynamics in 1979–2016 Observed from ESA CCI SM Dataset," *Water,* vol. 11, no. 5, p. 883, 2019.

[25] R. D. Magagi and Y. H. Kerr, "Retrieval of soil moisture and vegetation characteristics by use of ERS-1 wind scatterometer over arid and semi-arid areas," *Journal of Hydrology,* vol. s 188–189, no. 1, pp. 361-384, 1997.

[26] S. Hahn and W. Wagner, "Characterisation of Calibration-Related Errors of the Initial METOP ASCAT Soil Moisture Product," in *Geophysical Research Abstracts*, 2011, vol. 13, no. EGU2011-3178.

[27] S. Paloscia, G. Macelloni, E. Santi, and T. Koike, "A multifrequency algorithm for the retrieval of soil moisture on a large scale using microwave data from SMMR and SSM/I satellites," *IEEE Transactions on Geoscience & Remote Sensing,* vol. 39, no. 8, pp. 1655-1661, 2001.

[28] K. D. Ridder, "Surface soil moisture monitoring over Europe using Special Sensor Microwave/Imager (SSM/I) imagery," *Journal of Geophysical Research,* vol. 108, no. D14, p. 4422, 2003.

[29] M. Drusch, "Initializing numerical weather prediction models with satellite‐derived surface soil moisture: Data assimilation experiments with ECMWF's Integrated Forecast System and the TMI soil moisture data set," *Journal of Geophysical Research: Atmospheres,* vol. 112, no. D3, 2007.

[30] S. Chen, D. She, L. Zhang, M. Guo, and X. Liu, "Spatial Downscaling Methods of Soil Moisture Based on Multisource Remote Sensing Data and Its Application," *Water,* vol. 11, no. 7, p. 1401, 2019.

[31] L. Li *et al.*, "WindSat Global Soil Moisture Retrieval and Validation," *IEEE Transactions on Geoscience & Remote Sensing,* vol. 48, no. 5, pp. 2224-2241, 2010.

[32] Y. H. Kerr, P. Waldteufel, J.-P. Wigneron, J. Martinuzzi, J. Font, and M. Berger, "Soil moisture retrieval from space: The Soil Moisture and Ocean Salinity (SMOS) mission," *IEEE transactions on Geoscience and remote sensing,* vol. 39, no. 8, pp. 1729-1735, 2001.

[33] W. Jing, J. Song, and X. Zhao, "A Comparison of ECV and SMOS Soil Moisture Products Based on OzNet Monitoring Network," *Remote Sensing,* vol. 10, no. 5, p. 703, 2018, doi: 10.3390/rs10050703.

[34] W. A. Dorigo *et al.*, "Evaluation of the ESA CCI soil moisture product using ground-based observations," *Remote Sensing of Environment,* vol. 162, no. 2, pp. 380-395, 2015.

[35] A. Mcnally, S. Shukla, K. R. Arsenault, S. Wang, C. D. Peterslidard, and J. P. Verdin, "Evaluating ESA CCI soil moisture in East Africa," *International Journal of Applied Earth Observation & Geoinformation,* vol. 48, pp. 96-109, 2016.

[36] A. Gonzalez-Zamora, N. Sanchez, M. Pablos, and J. Martinez-Fernandez, "CCI soil moisture assessment with SMOS soil moisture and in situ data under different environmental conditions and spatial scales in Spain," *Remote Sensing of Environment,* vol. 225, pp. 469-482, 2019.

[37] C. Cui *et al.*, "Soil Moisture Mapping from Satellites: An Intercomparison of SMAP, SMOS, FY3B, AMSR2, and ESA CCI over Two Dense Network Regions at Different Spatial Scales," *Remote Sensing,* vol. 10, no. 2, p. 33, 2017, doi: 10.3390/rs10010033.

[38] P. Du *et al.*, "Advances of Four Machine Learning Methods for Spatial Data Handling: a Review," *Journal of Geovisualization and Spatial Analysis,* vol. 4, no. 13, pp. 1-25, 2020, doi: 10.1007/s41651-020-00048-5.

[39] H. Su, Y. Yu, Q. Du, and P. Du, "Ensemble Learning for Hyperspectral Image Classification Using Tangent Collaborative Representation," *IEEE Transactions on Geoscience and Remote Sensing,* pp. 1-13, 2020, doi: 10.1109/TGRS.2019.2957135.

[40] Y. Liu, W. Jing, Q. Wang, and X. Xia, "Generating high-resolution daily soil moisture by using spatial downscaling techniques: a comparison of six machine learning algorithms," *Advances in Water Resources,* vol. 141, p. 103601, 2020/07/01/ 2020, doi: https://doi.org/10.1016/j.advwatres.2020.103601.

[41] Y. Liu, Y. Yang, W. Jing, and X. Yue, "Comparison of Different Machine Learning Approaches for Monthly Satellite-Based Soil Moisture Downscaling over Northeast China," *Remote Sensing,* vol. 10, no. 2, p. 31, 2018.

[42] Y. Y. Liu *et al.*, "Developing an improved soil moisture dataset by blending passive and active microwave satellite-based retrievals," *Hydrology and Earth System Sciences (HESS) & Discussions (HESSD),* 2011. [Online]. Available: http://www.hydrol-earth-syst-sci.net/15/425/2011/hess-15-425-2011.html.

[43] Y. Y. Liu *et al.*, "Trend-preserving blending of passive and active microwave soil moisture retrievals," *Remote Sensing of Environment,* vol. 123, no. 3, pp. 280-297, 2012.

[44] Y. Bao, F. Mao, J. Min, D. Wang, and J. Yan, "Retrieval of bare soil moisture from FY-3B/MWRI data," *Remote Sensing for Land & Resources,* 2014.

[45] S. Wu and J. Chen, "Instrument performance and cross calibration of FY-3C MWRI," in *2016 IEEE International Geoscience and Remote Sensing Symposium (IGARSS)*, 2016: IEEE, pp. 388-391.

[46] D. Entekhabi *et al.*, "The Soil Moisture Active Passive (SMAP) Mission," *Proceedings of the IEEE,* vol. 98, no. 5, pp. 704-716, 2010, doi: 10.1109/jproc.2010.2043918.

[47] C. Dandridge, B. Fang, and V. Lakshmi, "Downscaling of SMAP Soil Moisture in the Lower Mekong River Basin," *Water,* vol. 12, no. 1, p. 56, 2020.

[48] S. K. Chan *et al.*, "Assessment of the SMAP Passive Soil Moisture Product," *IEEE Transactions on Geoscience & Remote Sensing,* vol. 54, no. 8, pp. 4994-5007, 2016.

[49] P. Ming, X. Cai, N. Chaney, D. Entekhabi, and E. F. Wood, "An Initial Assessment of SMAP Soil Moisture Retrievals Using High Resolution Model Simulations and In-situ Observations: SMAP Comparisons," *Geophysical Research Letters,* vol. 43, no. 18, pp. 9662-9668, 2016.

[50] S. Y. Mei, J. P. Walker, A. Monerris, C. Rüdiger, and T. J. Jackson, "On the identification of representative in situ soil moisture monitoring stations for the validation of SMAP soil moisture products in Australia," *Journal of Hydrology,* vol. 537, pp. 367-381, 2016.

[51] A. Chakravorty, B. R. Chahar, O. P. Sharma, and C. T. Dhanya, "A regional scale performance evaluation of SMOS and ESA-CCI soil moisture products over India with simulated soil moisture from MERRA-Land," *Remote Sensing of Environment,* vol. 186, pp. 514-527, 2016.

[52] H. Ma, J. Zeng, N. Chen, X. Zhang, M. H. Cosh, and W. Wang, "Satellite surface soil moisture from SMAP, SMOS, AMSR2 and ESA CCI: A comprehensive assessment using global ground-based observations," *Remote Sensing of Environment,* vol. 231, p. 111215, 2019.

[53] A. Gruber, W. A. Dorigo, W. Crow, and W. Wagner, "Triple Collocation-Based Merging of Satellite Soil Moisture Retrievals," *IEEE Transactions on Geoscience and Remote Sensing,* vol. 55, no. 12, pp. 6780-6792, 2017, doi: 10.1109/TGRS.2017.2734070.

[54] A. Gruber, T. Scanlon, R. v. d. Schalie, W. Wagner, and W. Dorigo, "Evolution of the ESA CCI Soil Moisture climate data records and their underlying merging methodology," *Earth System Science Data,* vol. 11, no. 2, pp. 717-739, 2019.

[55] R. Llamas, M. Guevara, D. Rorabaugh, M. Taufer, and R. Vargas, "Spatial Gap-Filling of ESA CCI Satellite-Derived Soil Moisture Based on Geostatistical Techniques and Multiple Regression," *Remote Sensing,* vol. 12, no. 4, p. 665, 2020.

[56] Y. Liu, Y. Yang, W. Jing, and X. Yue, "Comparison of Different Machine Learning Approaches for Monthly Satellite-Based Soil Moisture Downscaling over Northeast China," *Remote Sensing,* vol. 10, no. 2, p. 31, 2017, doi: 10.3390/rs10010031.

[57] D. Entekhabi *et al.*, "The Soil Moisture Active Passive (SMAP) Mission," *Proceedings of the IEEE,* vol. 98, no. 5, pp. 704-716, 2010.

[58] Y. Chen *et al.*, "Evaluation of SMAP, SMOS, and AMSR2 soil moisture retrievals against observations from two networks on the Tibetan Plateau," *Journal of Geophysical Research Atmospheres,* vol. 122, no. 11, pp. 5780–5792, 2017.

[59] S. Sabaghy, J. P. Walker, L. J. Renzullo, and T. J. Jackson, "Spatially enhanced passive microwave derived soil moisture: Capabilities and opportunities," *Remote Sensing of Environment,* vol. 209, no. C, pp. 551-580, 2018.

[60] W. A. Dorigo *et al.*, "The International Soil Moisture Network: A data hosting facility for global in situ soil moisture measurements," *Hydrology and Earth System Sciences,* vol. 15, no. 5, pp. 1675-1698, 2011.

[61] N. Sanchez, J. Martínez-Fernández, A. Scaini, and C. Perez-Gutierrez, "Validation of the SMOS L2 soil moisture data in the REMEDHUS network (Spain)," *IEEE Transactions on Geoscience and Remote Sensing,* vol. 50, no. 5, pp. 1602-1611, 2012.

[62] C. Albergel *et al.*, "An evaluation of ASCAT surface soil moisture products with in-situ observations in Southwestern France," *Hydrology & Earth System Sciences Discussions,* vol. 13, no. 4, pp. 115-124, 2009.

[63] J. Zeng, K.-S. Chen, H. Bi, and Q. Chen, "A preliminary evaluation of the SMAP radiometer soil moisture product over United States and Europe using ground-based measurements," *IEEE Transactions on Geoscience and Remote Sensing,* vol. 54, no. 8, pp. 4929-4940, 2016.

[64] K. H. Jensen and T. H. Illangasekare, "HOBE: A Hydrological Observatory," (in English), *Vadose Zone Journal,* vol. 10, no. 1, pp. 1-7, 2011, doi: 10.2136/vzj2011.0006.

[65] K. Dabrowska-Zielinska *et al.*, "Soil Moisture in the Biebrza Wetlands Retrieved from Sentinel-1 Imagery," *Remote Sensing,* vol. 10, no. 12, p. 1979, 2018. [Online]. Available: https://www.mdpi.com/2072-4292/10/12/1979.

[66] H. Bogena *et al.*, "TERENO – A new Network of Terrestrial Observatories for Environmental Research," *Migraciones Internacionales,* vol. 6, no. 3, pp. 109-138, 2007.

[67] I. Sandric, A. Diamandi, N. Oana, D. Saizu, C. Vasile, and B. Lucaschi, "VALIDATION AND UPSCALING OF SOIL MOISTURE SATELLITE PRODUCTS IN ROMANIA," *Int. Arch. Photogramm. Remote Sens. Spatial Inf. Sci.,* vol. XLI-B2, pp. 313-317, 2016, doi: 10.5194/isprs-archives-XLI-B2-313-2016.

[68] J.-C. Calvet, N. Fritz, F. Froissard, D. Suquia, A. Petitpa, and B. Piguet, "In situ soil moisture observations for the CAL/VAL of SMOS: The SMOSMANIA network," in *2007 IEEE International Geoscience and Remote Sensing Symposium*, 2007: IEEE, pp. 1196-1199.

[69] J. Benesty, J. Chen, Y. Huang, and I. Cohen, *Pearson Correlation Coefficient*. 2009.

[70] R. H. Reichle and R. D. Koster, "Bias reduction in short records of satellite soil moisture," *Geophysical Research Letters,* vol. 31, no. 19, 2004.

[71] S.-B. Kim *et al.*, "Surface soil moisture retrieval using the l-band synthetic aperture radar onboard the soil moisture active–passive satellite and evaluation at core validation sites," *IEEE Transactions on Geoscience and Remote Sensing,* vol. 55, no. 4, pp. 1897-1914, 2017.

[72] G. Vachaud, A. P. D. Silans, P. Balabanis, and M. Vauclin, "Temporal Stability of Spatially Measured Soil Water Probability Density Function 1," *Soil Science Society of America Journal,* vol. 49, no. 4, pp. 822-828, 1985.

[73] M. Mirzargar, R. T. Whitaker, and R. M. Kirby, "Curve Boxplot: Generalization of Boxplot for Ensembles of Curves," *IEEE Transactions on Visualization and Computer Graphics,* vol. 20, no. 12, pp. 2654-2663, 2014.

[74] J. R. Piepmeier *et al.*, "Radio-Frequency Interference Mitigation for the Soil Moisture Active Passive Microwave Radiometer," *IEEE Transactions on Geoscience & Remote Sensing,* vol. 52, no. 1, pp. 761-775, 2014.

[75] B. P. Mohanty, M. H. Cosh, V. Lakshmi, and C. Montzka, "Soil moisture remote sensing: State-of-the-science," *Vadose Zone Journal,* vol. 16, no. 1, 2017.

[76] H. Mao, D. Kathuria, N. Duffield, and B. P. Mohanty, "Gap Filling of High-Resolution Soil Moisture for SMAP/Sentinel-1: A Two-layer Machine Learning-based Framework," *Water Resources Research,* vol. 55, no. 8, pp. 6986-7009, 2019.

[77] K. Fang, C. Shen, D. Kifer, and X. Yang, "Prolongation of SMAP to spatiotemporally seamless coverage of continental US using a deep learning neural network," *Geophysical Research Letters,* vol. 44, no. 21, pp. 11,030-11,039, 2017.

[78] A. Al-Yaari *et al.*, "Evaluating soil moisture retrievals from ESA's SMOS and NASA's SMAP brightness temperature datasets," *Remote Sensing of Environment,* vol. 193, pp. 257-273, 2017.

[79] M. Spencer *et al.*, "The Soil Moisture Active Passive (SMAP) mission L-Band radar/radiometer instrument," presented at the Geoscience and Remote Sensing Symposium (IGARSS), 2010 IEEE International, 2010.

[80] A. Colliander *et al.*, "Validation of SMAP surface soil moisture products with core validation sites," *Remote Sensing of Environment,* vol. 191, pp. 215-231, 2017, doi: 10.1016/j.rse.2017.01.021.

[81] J. R. Piepmeier *et al.*, "Radio-frequency interference mitigation for the soil moisture active passive microwave radiometer," *IEEE Transactions on Geoscience and Remote Sensing,* vol. 52, no. 1, pp. 761-775, 2013.